COMPUTATIONAL METHODS IN APPLIED MATHEMATICS, Vol. 7 (2007), No. 2, pp. 103–117

SIMULATION OF INTERACTING DISCONTINIOUS SOLUTIONS ON DYNAMICALLY ADAPTIVE GRIDS

P. V. BRESLAVSKY[1] AND V. I. MAZHUKIN[1]

Abstract — A further development of the dynamic adaptation method for gas dynamic problems describing multiple interactions of the shock waves, rarefaction waves, and contact boundaries are considered. By the test Woodward — Colella problem the efficiency of the proposed method for solving problems of gas dynamics with explicit definition of shock waves and contact boundaries is shown. For the problem solution mechanism of the adaptation of diffusion type is used. A choice of the adaptation coefficient for obtaining solution in each of subdomains of quasiuniform grid is substantiated. The discontinuities interaction between each other is solved by the Riemann problem. Application of the dynamic adaptation method allowed obtaining solution in 420 cells which practically coincides with the results of WENO5m method in 12800 cells.

2000 Mathematics Subject Classification: 65N50; 65N30.

Keywords: gas dynamics problems, numerical dynamic grid adaptation method, multiple interaction of shock waves and rarefaction waves, contact discontituities.

Introduction

The last few decades have seen a further development of solution methods for systems of equations of the hyperbolic type and, as consequence, of gas dynamic equations. The rapid progress in this area is indicative of enhanced interest in this matter, since there exists a large number of practical problems that are simulated by systems of differential equations of the hyperbolic type.

The existing solution methods for gas dynamic problems can arbitrarily be subdivided into two classes: shock-capturing methods and explicit-boundary-tracking methods. Each of them has its own advantages and disadvantages.

The shock-capturing methods, in which the problem is solved, as a rule, in invariable initially specified domain, permit calculations without taking into account the specific features that arise inside this domain. Precisely this fact determines the main advantages and disadvantages of the above methods. On the one hand, the shock-capturing methods are easy to realize computationally, since they have a simple algorithmic part, and on the other hand, they are unable to reliably describe the weak and strong discontinuities arising in the solution process. By the reliability is meant in this case the presence of just discontinuities in the solution domain rather than their smoothed analogs. Initially, this smoothness was attained due to the introduction into the model of artificial viscosity (linear, quadratic, and their combination). Recently, the use of artificial viscosity looks as some anachronism. This is due, not in the last place, to the fact that new algorithms for solving gas dynamic problems with discontinuity smoothness have been developed.

[1] *Institute of mathematical modeling RAS*, Miusskaya pl. 4, Moscow, 125047 Russia. E-mail: immras@orc.ru

The major problem in constructing difference schemes in the shock-capturing methods is the desire to increase the approximation accuracy and simultaneously obtain monotonic numerical solutions, which in the presence of strong and weak discontinuities is a nontrivial problem. Godunov's theorem [8] states that in a linear case monotonicity can be provided only in difference schemes of the first order of approximations. In the 1970s, the development of "monotonized" difference schemes of a higher order of accuracy was associated with the works of Van Leer [30] and the flux-correction antidiffusion method (FCT-method) of Boris and Book [3,24]. The next stage in the development of difference schemes for solving type is the appearance of TVD schemes (see, for example, the works of Harten [9], Osher [25]) and the development of ENO and WENO methods [10,20]. Another direction, which is essentially similar to the above methods, is based on monotone or quasi-monotone interpolation of grid solutions. It is possible to term the methods using this technique as grid-solution-reconstruction methods. In the foreign literature, finite parabolic reconstruction — the so-called PPM (piecewise parabolic method) is the most popular [6]. The existing solution methods for gas-dynamic problems are described in more detail in [16] or [2].

The main disadvantages of all shock-capturing methods are the use of a too large number of grid nodes for achieving the required accuracy, the application of complex methods of node crowding at the sites of large gradients, and the impossibility of solving them with the use of problems that require definition of discontinuities (e.g., problems in which an accurate account of the kinetics at the boundaries is required).

The explicit-discontinuity-tracking methods [12, 17, 31], despite their certain disadvantages, among which is the absence of a priori information about the place where a discontinuity arises or the difficulty of tracking the geometry of the domains in multidimensional statements, show undoubted advantages for a wide class of problems. In the last few years, the most extensively used method has been that known the front tracking method [17, 29] which is emplyed, as a rule, together with AMR (adaptive mesh refinement) algorithms based on Euler grids. It might be well to point out the active development of solution methods for gas dynamic problems adaptive for gradients and explicitly tracked discontinuities on moving grids, among which are the variation methods [14], the harmonic-map method [18], and dynamic-adaptation method [7]. The adaptation problems for multidimensional meshes are fairly closely allied to the problem of constructing computational meshes for arbitrary simply connected regions. One can familiarize himself with some of approaches to the solution of this problems and the difficulties arising therewith, e.g., in reviews [13] and [19]. In [1], the calculation of the detonation waves with the tracking of a heating-up shock wave is performed on adaptive grids crowding in the vicinity of large solution gradients. To construct a grid, at each instant of time the Dirichlet functional minimization problem is stated. The variational principle of grid construction is the most popular at the present time and is often used to construct initial grids for complex domains [14]. However, if the calculation domains changes considerably in the solution process, then one has to face now and then the basic problem of the variational methods consisting in that "in extreme situations the majority of algorithms generate grids whose cells can be turned out, and even situations are possible where the grid nodes go beyond the domain boundaries" [13].

The dynamic adaptation method considered in the present paper is based on the transition to an arbitrary nonstationary coordinate system; in the unknowns are not only the grid functions, but also the coordinates of the grid nodes. The transformation of coordinates is conducted with the use of the sought solution and, depending on the solution peculiarity; a particular distribution of grid nodes is obtained [4, 5, 7, 22]. The above approach makes

it possible to perform calculations by both the shock-capturing methods with automatic crowding of nodes to the solution singularities and the methods with explicit tracking of moving boundaries and discontinuities, when required. Both these techniques were used earlier to investigate the uniformly-accelerating-piston problem [5].

Examples of solving multidimensional problems by means of the dynamic-adaptation method are given, e.g., in [21, 27].

The aim of the present work is to develop further the dynamic-adaptation method for gas-dynamic problems describing the multiple interactions of shock waves, rarefaction waves, and contact boundaries.

The peculiarities of the dynamic-adaptation method are shown with the example of solving the Woodward — Collela test problem [6], which is now the most popular test for all new solution methods for gas dynamic problems.

The major problems in the example under consideration are connected with the tracking of discontinuities and their interaction. Discontinuity tracking calls for the development of a reliable means for determining the moment and location of the arising discontinuity. Multiple interactions between discontinuities are characterized by a great diversity, but it can be reduced to several elementary interactions: collision of two couterrunning shock waves, absorption of one shock wave by another wave overtaking it, and passage of the shock wave through the contact boundary.

1. Woodward — Collela problem [6]

The Woodward — Collela problem describes the interaction of two couterrunning detonation waves resulting from the decomposition of two arbitrary discontinuities (Figs. 1.1 and 1.2). Mathematically, the problem is reduced to the solution of the system of gas dynamic equations: the differential laws of conservation of mass, momentum, and energy, complemented with initial and boundary conditions adequate for each of the problems. In the Euler coordinate system in one-dimensional statement, the problem is formulated in the following form:

$$\begin{cases} \dfrac{\partial \rho}{\partial t} + \dfrac{\partial}{\partial x}(\rho u) = 0, \\ \dfrac{\partial}{\partial t}(\rho u) + \dfrac{\partial}{\partial x}\left(P + \rho u^2\right) = 0, \qquad P = \rho R T, \quad \varepsilon = \dfrac{R}{\gamma - 1} T, \quad \gamma = 1.4, \\ \dfrac{\partial}{\partial t}(\rho \varepsilon) + \dfrac{\partial}{\partial x}(\rho u \varepsilon) + P \dfrac{\partial u}{\partial x} = 0, \end{cases}$$

$$t \geqslant 0, \quad x_\ell \in [0,\ 0.1)\,, \quad x_m \in (0.1 \div 0.9)\,, \quad x_r \in (0.9 \div 1]\,, \tag{1.1}$$

By the data in the initial state gas exists in three ℓ, m, r regions in three different states:

$$t = 0: \quad \begin{pmatrix} \rho \\ u \\ P \end{pmatrix}_\ell = \begin{pmatrix} 1 \\ 0 \\ 10^3 \end{pmatrix}, \quad \begin{pmatrix} \rho \\ u \\ P \end{pmatrix}_m = \begin{pmatrix} 1 \\ 0 \\ 10^{-2} \end{pmatrix}, \quad \begin{pmatrix} \rho \\ u \\ P \end{pmatrix}_r = \begin{pmatrix} 1 \\ 0 \\ 10^2 \end{pmatrix}. \tag{1.2}$$

At the boundaries $x = 0$, and $x = 1$ impermeability condition $u(t, 0) = u(t, 1) = 0$ is given. At the initial instant of time two arbitrary discontinuities are set to the points $x = 0.1$ and $x = 0.9$, Fig. 1.1.

Notation: ρ — density, u — velocity, P — pressure, ε, T — internal energy and temperature, R — gas constant, γ — adiabatic index, x_ℓ, x_m, x_r — dimensions of ℓ, m, r — regions.

The decomposition of arbitrary discontinuities situated at points $x = \{0.1, 0.9\}$ (Fig. 1.1) leads to the formation in the regions adjoining these points of a complex structure containing rarefaction waves, contact discontinuities, and shock waves (Fig. 1.2). In order to determine this structure, it is necessary to solve, prior to calculations, an additional problem — the so-called arbitrary discontinuity decomposition problem. Analysis of its solution for ideal gas can be found, e.g., in [26, 28]. As applied to the present study, in the case of equations of state for ideal gas and discontinuity decomposition of two types — diverging shock waves and diverging shock wave and rarefaction wave joining each other through the contact boundary — the following algorithm can be written.

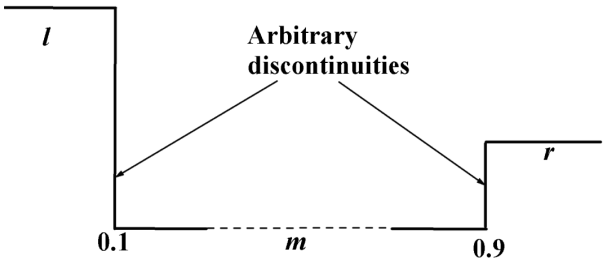

Fig. 1.1. Scheme profile of pressure and temperature at the initial time in the Woodward — Collela problem

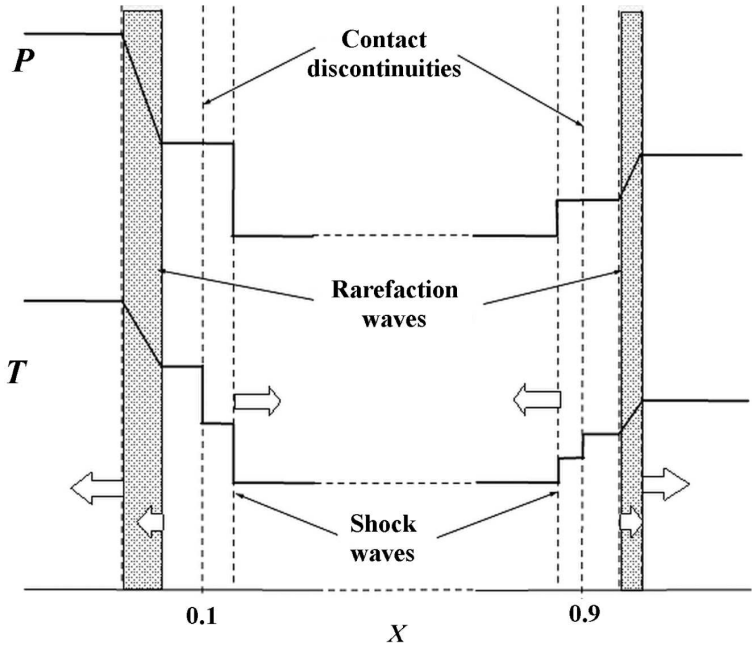

Fig. 1.2. Scheme of the decomposition of arbitrary discontinuities at the initial time (pressure P and temperature T profiles; the regions of rarefaction waves are shaded); arrows show the directions of motion of fronts

Let $n = 1$ correspond to parameters P_1, u_1, ρ_1, T_1 on the left side of the arbitrary discontinuity, and $n = 2$ — to parameters P_2, u_2, ρ_2, T_2 on the right side. It is required to find parameters $P_3 = P_4$, $u_3 = u_4$, ρ_3, ρ_4, T_3, T_4 upon decomposition, where *3 – 4* is a contact boundary that separates the gas in state *3* adjoining on the other side wave *1 – 3* and the gas in state *4* with the second boundary corresponding to wave *4 – 2*. By virtue of the self-similarity of the solution of the discontinuity decomposition problem, as shown in [26, 28], waves *1 – 3* and *2 – 4*, if any, represent either a shock wave or a rarefaction wave. Therefore, if $P_1 < P_3$, then *1 – 3* is a shock wave. In this case, the parameters P_3, u_3 are determined in a one-to-one manner from the Hugoniot adiabat that passes through the point P_1, u_1. But

if, vice versa, $P_1 > P_3$, then *1 – 3* is a rarefaction wave. Then the parameters P_3, u_3 of state 3 are found by means of the Poisson adiabat that passes through the point P_1, u_1. The type of wave *4 – 2* as a function of P_2, P_4 is determined in a similar manner. Proceeding from the foregoing, let us define the function $F_n(P)$ for each state *1* of the arbitrary discontinuity under consideration.

$$F_n(P)=\begin{cases} P_n+\dfrac{\gamma+1}{4}\left[\rho_n\left(u_3-u_n\right)^2+\sqrt{\rho_n^2\left(u_3-u_n\right)^4+\dfrac{16\gamma}{(\gamma+1)^2}P_n\rho_n\left(u_3-u_n\right)^2}\right], & P>P_n, \\ P_n\left[1-\dfrac{\gamma-1}{2\sqrt{\gamma P_n/\rho_n}}(u_3-u_n)\right]^{2\gamma/(\gamma-1)}, & P<P_n, \end{cases} \tag{1.3}$$

In this definition of the function, the first equation describes the Hugoniot adiabat, and the second one — Poisson adiabat. Equating $F_1(P)$ and $F_2(P)$, from the values of P_1, u_1, ρ_1, P_2, u_2, ρ_2 on the discontinuity, let us find by the Newton method the gas-dynamic velocity $u_3 = u_4$ at the contact boundary. Upon calculation of $u_3 = u_4$ let us determine $P_3 = P_4$ and then the other quantities: densities ρ_3, ρ_4 and temperatures T_3, T_4, and in the presence of shock waves, using the Hugoniot conditions, the discontinuity velocities:

$$\begin{cases} \rho_0\left(u_0-D_x\right)=\rho_1\left(u_1-D_x\right)=Q_x, \\ P_0+\rho_0\left(u_0-D_x\right)^2=P_1+\rho_1\left(u_1-D_x\right)^2, \\ \varepsilon_0+\dfrac{P_0}{\rho_0}+\dfrac{(u_0-D_x)^2}{2}=\varepsilon_1+\dfrac{P_1}{\rho_1}+\dfrac{(u_1-D_x)^2}{2}. \end{cases} \tag{1.4}$$

Subscripts 0 and 1 pertain to parameters on different sides of a discontinuity; D_x and Q_x denote the mass velocity and flow through the boundary. Solving the decomposition of two arbitrarily given discontinuities by means of the above algorithm, we obtain the following structure (Fig. 1.2). At the site of initial discontinuities contact boundaries are situated, and in the direction to the outer boundaries of the region rarefaction waves propagate, and shock waves propagate counter to each other.

Mathematically, this fact can be written as follows:

$$t\approx 0\colon \begin{cases} x\in[0,0.099] & \rho=1,\quad u=0,\quad P=10^3, \\ x\in(0.099,0.0995) & f(x)=f(0.099)+(x-0.099)(f(0.0995)-f(0.099))/0.0005, \\ x\in[0.0995,0.1) & \rho=0.59,\quad u=19.5976,\quad P=4.609\cdot 10^2, \\ x\in(0.1,0.101) & \rho=5.99924,\quad u=19.5976,\quad P=4.609\cdot 10^2, \\ x\in(0.101,0.899) & \rho=1,\quad u=0,\quad P=10^{-2}, \\ x\in(0.899,0.9) & \rho=5.99242,\quad u=-6.1964,\quad P=4.609\cdot 10^1, \\ x\in(0.9,0.9005] & \rho=0.583,\quad u=-6.1964,\quad P=4.609\cdot 10^1, \\ x\in(0.9005,0.901) & f(x)=f(0.9005)+(x-0.9005)(f(0.901)-f(0.9005))/0.0005, \\ x\in[0.901,1] & \rho=1,\quad u=0,\quad P=10^2, \end{cases} \tag{1.5}$$

where $f(x)$ is any gas-dynamic function (ρ, u, P) determined by the formula of linear interpolation for x in the interval stated. At the initial instant of time at the contact boundaries

$x = 0.1$ and $x = 0.9$ fulfillment of the conditions $u_0 = u_1$, $P_0 = P_1$ is assumed, and at points $x = 0.101$ and $x = 0.899$ two shock waves reside, for which the Hugoniot conditions (1.4) are fulfilled.

2. Solution method

Using substitution of variables of the general form, in accordance with the dynamic adaptation method, we make a transition to an arbitrary nonstationary coordinate system with variables (q, τ), in which the system of equations (1.1) will be written as follows [5]:

$$\begin{cases} \dfrac{\partial}{\partial\tau}\left(\dfrac{\psi}{\rho}\right) + \dfrac{\partial}{\partial q}\left(\dfrac{Q}{\rho} - u\right) = 0, \\ \dfrac{\partial}{\partial\tau}(\psi u) + \dfrac{\partial}{\partial q}(P + Qu) = 0, \\ \dfrac{\partial}{\partial\tau}(\psi\varepsilon) + \dfrac{\partial}{\partial q}(Q\varepsilon) + P\dfrac{\partial u}{\partial q} = 0, \\ \dfrac{\partial\psi}{\partial\tau} = -\dfrac{\partial Q}{\partial q}, \quad \dfrac{\partial x}{\partial q} = \dfrac{\psi}{\rho}, \end{cases} \quad P = \rho RT, \quad \varepsilon = \frac{R}{\gamma - 1}T, \quad \gamma = 1.4, \quad \tau \geqslant 0, \quad q \in [0, 1], \quad (2.1)$$

where ψ/ρ is a transform Jacobian, Q is a transform function, whose physical meaning is the flow of matter through the boundary, $\partial x/\partial t = -Q/\rho$ is the velocity of the coordinate system.

As a result, in the variables (q, τ) we have obtained an augmented differential system (6), in which the last differential equation is an equation of inverse transformation, which together with the transform Jacobian is used to determine the coordinates of grids nodes, i.e., to construct a calculation grid. Controlled distribution of nodes for each instant of time is carried out by means of the transform function Q, whose concrete form is to be determined.

When $\psi = \rho$ is chosen, the transform Jacobian becomes equal to unity, and, consequently, the coordinates in the physical and calculated spaces at the beginning of the calculation will coincide with each other. Therefore, the initial equations (1.5) in the variables (q, τ) remain unaltered and are not given to avoid repetition.

In the calculated space, the boundaries $q = 0$ and $q = 1$ are fixed and impenetrable

$$u(\tau, 0) = Q(\tau, 0) = 0, \quad u(\tau, 1) = Q(\tau, 1) = 0. \quad (2.2)$$

The flow of matter through the contact boundaries $q = 0$ and $q = 1$ is absent. Consequently,

$$u_0(\tau, 0.1) = u_1(\tau, 0.1), \quad P_0(\tau, 0.1) = P_1(\tau, 0.1), \quad Q(\tau, 0.1) = 0,$$

$$u_0(\tau, 0.9) = u_1(\tau, 0.9), \quad P_0(\tau, 0.9) = P_1(\tau, 0.9), \quad Q(\tau, 0.9) = 0. \quad (2.3)$$

The boundaries $q = 0.101$ and $q = 0.899$ are claimed to be moving and are separated explicitly. The velocity of their motion is estimated from the conservation flow (1.4).

3. Solution structure

In the evolution of the given problem, three basic points can be distinguished.

1) Decomposition of two arbitrary discontinuities in the vicinity of the outer boundaries of the region under consideration (Fig. 1.1) and, as a consequence, the appearance at the sites of decompositions of contact boundaries, from which rarefaction waves propagate towards the outer boundaries, and two shock waves with different intensities propagate towards each other (Fig. 1.2).

2) Collision of these shock waves leading to the formation of a contact boundary with shock waves moving away from it.

3) Passage of one of the shock waves through a contact boundary, as a result of which a rarefaction wave will move away from the contact boundary in the direction opposite to the direction of propagation of the shock wave.

Since in the given problem two arbitrary discontinuities were given initially, to employ the method of dynamic adaptation with explicit tracking of boundaries, one has to solve at the initial stage the problem of arbitrary discontinuity decomposition [26, 28]. As a result of the solution, instead of one arbitrary discontinuity a contact boundary will appear, from which a shock wave propagates into the region of the problem, and a rarefaction wave propagates in the opposite direction (Fig. 1.2). In the present study, rarefaction waves are not separated explicitly, while it should be noted that, if necessary, the algorithm with the separation of both the outer and inner boundaries of the rarefaction wave can be realized. In view of the foregoing, the initially given discontinuity is replaced by two explicitly separated ones - a contact boundary and a shock wave. The characteristic density profile is shown in Fig. 3.1.

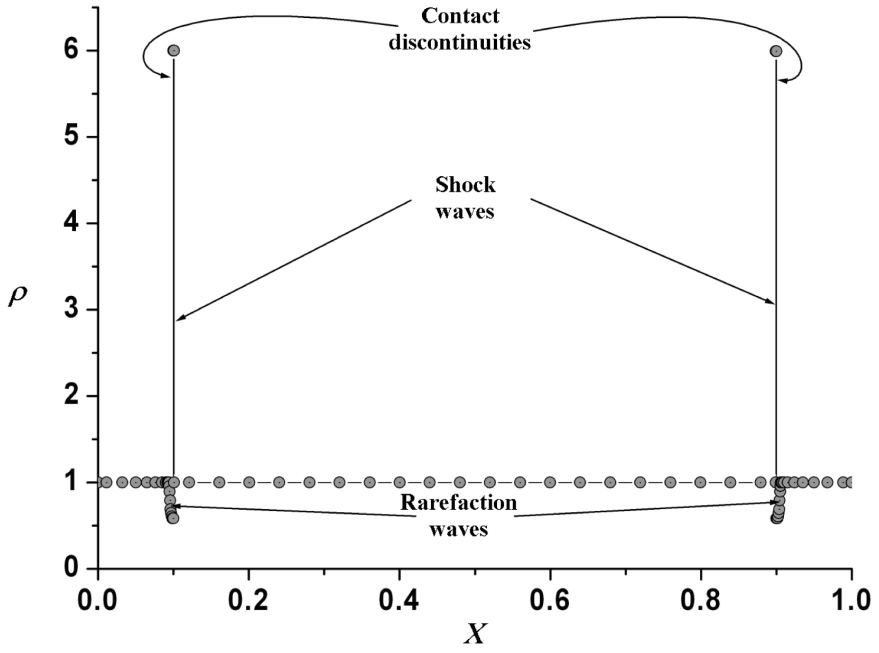

Fig. 3.1. Density profile at the beginning of calculation

In the solution process, the shock waves running towards each other will collide. Their interaction will lead to the formation of a contact boundary and two shock waves moving away from it. This situation is also simulated as the decomposition of an arbitrary discontinuity with parameters corresponding to the gas-dynamic characteristics after the shock wave fronts. Mathematically, this collision will lead to the appearance of one more additional calculated region because of the necessity to separate the contact boundary that has arisen (the calculation algorithm upon decomposition is considered in more detail in the next paragraph.

4. Arbitrary discontinuity decomposition

It is necessary to consider the problem of the arbitrary discontinuity decomposition in more detail, since it has to be solved not only in the case of initially given discontinuities. As mentioned above, any interactions of discontinuity solutions between one another are reduced to the solution of the arbitrary discontinuity decomposition problem. The algorithm for solving this problem was considered earlier. Using the $F_n(P)$ (1.3), one determines the values of the gas-dynamic velocity and the pressure on the contact boundary formed at the site of interaction of discontinuities. From the Hugoniot conditions and the equations of state the values of the density, the temperature, and the velocities of the shock waves formed are determined. The type of decomposition is uniquely determined from the relation between the pressure obtained and the pressure on the initially given discontinuity. Let us consider the following two situations:

1) the left shock wave passes through the right contact boundary; and

2) two counterrunning shock waves interact with each other.

In the first case, the obtained pressure satisfies the inequality $P_1 > P_3 = P_4 > P_2$, and the algorithm for continuing the calculation will be as follows: on the left, instead of the shock wave, a discontinuity contact appears, in which $u_3 = u_4$ and $P_3 = P_4$, as well as the values of ρ_3, T_3 on the left and ρ_4, T_4 on the right of discontinuity are given; the right boundary is replaced by a shock wave with the values of P_4, u_4, ρ_4, T_4 after the front and of P_2, u_2, ρ_2, T_2 before the front. In the region between discontinuities all gas-dynamic quantities are assumed to be equal to P_4, u_4, ρ_4, T_4. On the left of the contact boundary, an explicitly nonseparable rarefaction wave is located.

In the second case, the inequality $P_3 = P_4 > P_1 > P_2$ is fulfilled, which somewhat complicates the calculation algorithm. On the left boundary, instead of the shock wave moving from left to right, there appears a shock wave propagating in the opposite direction with the values of P_3, u_3, ρ_3, T_3 after the front and of P_1, u_1, ρ_1, T_1 before the front. On the right, instead of the shock wave, there appears a contact boundary, on which $u_3 = u_4$, $P_3 = P_4$ are given, and the values of ρ_3, T_3 on the left of the discontinuity and of ρ_4, T_4 on its right are given. Then an additional subregion is introduced, whose left boundary is a contact discontinuity and the right one - a shock wave with parameters P_4, u_4, ρ_4, T_4 after the front and P_2, u_2, ρ_2, T_2 before the front. In the region between the left shock wave and the contact boundary all gas-dynamic quantities are assumed to be equal to P_3, u_3, ρ_3, T_3, and between the contact boundary and the right shock wave — to P_4, u_4, ρ_4, T_4.

5. Choosing the adaptation function Q and solution

As mentioned above, for the desired distribution of grid nodes, the transform function Q should depend on the sought solution or its singularities. The main singularity of the solution of the problem of interaction of two counterrunning shock waves is the presence of moving boundaries. Preliminary analysis has shown that to solve this problem, it is enough to restrict oneself to the application of a grid that is quasi-uniform at each instant of time. A dynamic quasi-uniform distribution of nodes can be obtained by using of one of the simplest forms of the function Q obtained by means of the so-called diffusion approximation [4, 15].

$$Q = -D\frac{\partial \psi}{\partial q}, \tag{5.1}$$

where D is a free parameter having the meaning of the diffusion coefficient. Its value can be determined in terms of the problem parameters: geometric dimensions of the region and the velocity of motion of the boundaries [15]. The determination is based on the linear estimation of the zone covered by perturbations for differential equations of the parabolic type

$$L \approx \sqrt{D\Delta t}. \tag{5.2}$$

In (5.1), the coefficient D is chosen such that in time Δt the perturbation manages to cover the distance L equal to the distance between the moving boundaries. Expressing Δt in terms of the velocity of motion of boundaries υ $\Delta t = \Delta L/|\upsilon_\ell - \upsilon_r|$, the coefficient D can be given in the form $D = L^2|\upsilon_\ell - \upsilon_r|/\Delta L$, where $\Delta L = (\psi/\rho)L$ is the extension of the region in the time Δt, and υ_ℓ, υ_r are the velocities of motion of the left and right boundaries, respectively. In view of the expression for the velocity $\upsilon_{\ell,r} = -(Q/\rho)_{\ell,r}$ the coefficient D will be written in the final form as

$$D = \frac{|Q_\ell - Q_r|L}{\psi}. \tag{5.3}$$

In the discrete space of the grid functions, where the spatial step is h and the domain length is $L = hN$ is expressed in terms of the partitions number N, the coefficient D can be given in the form

$$D = \frac{|Q_\ell - Q_r|hN}{\psi_{\min}}. \tag{5.4}$$

Thus, the transform function Q turns out to be related to the singularities of the problem under consideration: with the dimension $L(t)$ and the velocity of motion of the domain boundaries $\upsilon_{\ell,r}$.

6. Difference approximation and solution algorithm

For numerical realization of model (2.1) – (5.4), in the calculated space a difference grid with integer and half-integer nodes

$$\omega = \left\langle \begin{array}{l} (q_i, \tau^j),\ (q_{i+1/2}, \tau^j),\ q_{i+1} = q_i + h,\ q_{i+1/2} = q_i + 0.5h, \quad i = 0, 1, \ldots, N-1 \\ \tau^{j+1} = \tau^j + \Delta\tau^j, \quad j = 0, 1, \ldots \end{array} \right\rangle$$

was introduced.

For approximation of the differential equations, the finite-difference method on diverse grids was used, and a family of difference schemes was written [5], in which at half-integer points the density $\rho_{i+1/2}$, the temperature $T_{i+1/2}$, the pressure $P_{i+1/2}$, and the internal energy $\varepsilon_{i+1/2}$ are determined, and at integer points the velocity u_i, the function Q_i, and the

coordinate x_i are determined.

$$\begin{cases} \dfrac{\psi^{j+1}_{i+1/2} - \psi^{j}_{i+1/2}}{\Delta\tau^j} = -\dfrac{Q^{\sigma_1}_{i+1} - Q^{\sigma_1}_{i}}{h_{i+1/2}}, \\ \dfrac{\psi^{j+1}_{i+1/2}/\rho^{j+1}_{i+1/2} - \psi^{j}_{i+1/2}/\rho^{j}_{i+1/2}}{\Delta\tau^j} = -\dfrac{Q^{\sigma_1}_{i+1}/\rho^{\sigma_2}_{i+1} - Q^{\sigma_2}_{i}/\rho^{\sigma_2}_{i} - u^{\sigma_3}_{i+1} + u^{\sigma_3}_{i}}{h_{i+1/2}}, \\ \dfrac{\psi^{j+1}_{i} u^{j+1}_{i} - \psi^{j}_{i} u^{j}_{i}}{\Delta\tau^j} = -\dfrac{P^{\sigma_4}_{i+1/2} - P^{\sigma_4}_{i-1/2} + Q^{\sigma_1}_{i+1/2} u^{\sigma_3}_{i+1/2} - Q^{\sigma_1}_{i-1/2} u^{\sigma_3}_{i-1/2}}{0.5(h_{i+1/2} + h_{i-1/2})}, \\ \dfrac{\psi^{j+1}_{i+1/2}\varepsilon^{j+1}_{i+1/2} - \psi^{j}_{i+1/2}\varepsilon^{j}_{i+1/2}}{\Delta\tau^j} = -\dfrac{Q^{\sigma_1}_{i+1}\varepsilon^{\sigma_5}_{i+1} - Q^{\sigma_1}_{i}\varepsilon^{\sigma_5}_{i}}{h_{i+1/2}} - P^{\sigma_4}_{i+1/2}\dfrac{u^{\sigma_3}_{i+1} - u^{\sigma_3}_{i}}{h_{i+1.2}}, \end{cases} \tag{6.1}$$

where $f^{\sigma_r} = \sigma_r \cdot f^{j+1} + (1 - \sigma_r) \cdot f^j$, and $\sigma_r = \sigma_1, \sigma_2, \ldots$ weighting factors defining the degree of implicitness of the deference scheme. If $\sigma_1 = \sigma_2 = \cdots = 0$, then we obtain a completely explicit difference scheme with an approximation error $O(\Delta\tau + h^2)$. In the case that $\sigma_1 = \sigma_2 = \cdots = 1$, the scheme is completely implicit with the same order of approximation. To the value of $\sigma_1 = \sigma_2 = \cdots = 0.5$ there correspond a scheme with an order of approximation $O(\Delta\tau^2 + h^2)$. Computations were performed for both a completely implicit difference scheme and a mixed scheme with weighting factors equal to 0.5. The choice of weights did not produce any appreciable influence on the results obtained, except for the value of the integration step $\Delta\tau$. This paper presents the results obtained for a completely implicit difference scheme with a first order of approximation in time and with a second order of approximation in space.

Since the class of difference schemes used to solve the problem belongs to implicit schemes with central space differences, in the case of convergence of the iteration cycle the difference schemes under consideration are absolutely stable and converge to the solution with the accuracy determined by the order of approximation [28]. According to the known Godunov theorem, monotone difference schemes with an order of approximation higher than the first order in space do not exist. Nevertheless, schemes of high orders of approximation are more preferable than the first order schemes, since in the case of smooth solutions they permit obtaining more exact solutions on spatial grids. Obviously, the difference schemes proposed in the present paper will not be monotone, since they have a second order of approximation in space and do not use any monotonization mechanism. It should be noted, however, that with the use of the dynamic adaptation method many of the problem singularities (shock waves and contact boundaries) are separated explicitly. From the regions with large gradients, which could influence the vacation of solution monotonicity, only rarefaction waves remain. The regions of rarefaction waves enlarge with time in space thus decreasing the initial gradients of the sought functions. This fact, as well as the controlled motion of the calculation grid nodes in the physical space consistent with the sought solution permit decreasing considerably the solution oscillations. Both of the above facts have made it possible to do without separation of the rarefaction wave boundaries and introduction into the difference scheme the monotonization procedure for the Woodward — Colella problem investigated in the present paper. It should be noted that the use of the dynamic adaptation method in no way contradicts the use of various difference schemes and monotone algorithms (e.g., TVD or WENO) for a wide class of problems, and is their essential complement in the cases where reconstruction of the calculation grid at the sites of solution singularities

is required. At the same time, as the present sudy shows, in a number of problems it is also possible to do without the monotonization algorithm developed. The main advantage of the dynamic adaptation method is that the problem of solution tracking and grid construction is formulated in the form of a single differential model, in which the mechanism of grid reconstruction is consistent with the sought solution (in each differential equation the metric function ψ and the adaptation function Q, whose interrelationship is reflected in the complement differential equation, is present). As was shown in [22] and [23], due to the motion of grid nodes consistent with the solution it is possible to considerably lower the dispersion of the difference schemes.

For the functions $\{u, Q\} = f$ given in integer grid nodes ω, their values in half-integer nodes were determined by the formula $f_{i+1/2} = 0.5(f_i + f_{i+1})$. Likewise, the values of the other functions $\{\psi, \rho, T, P, \varepsilon\} = f$ in integer nodes were determined from the known values of these functions in half-integer ones $f_i = 0.5(f_{i-1/2} + f_{i+1/2})$.

The algorithm for calculating the finite-difference equations (13) is schematically represented in Fig. 6.1 and consists in sequential iteration by the Newton method of two blocks, one of which contains a difference analog of the energy equation, and the second one — analogs of the equations of continuity and motion and the equation responsible for the reconstruction of the grid (of the first three equations of system (2.1)). Both blocks were involved in the global iteration cycle. In those cases where the number of external iterations of the global cycle exceeded 7 or the number of internal iterations turned out to be more than 10, the time step was halved. If the number of global operations became less than 4, then the next time step was increased by 20%. As the initial approximation for each of the sought grid function, the value of $f^{j+1^{(0)}} = f^j + (f^j - f^{j-1})\Delta\tau^j/\Delta\tau^{j-1}$ was chosen.

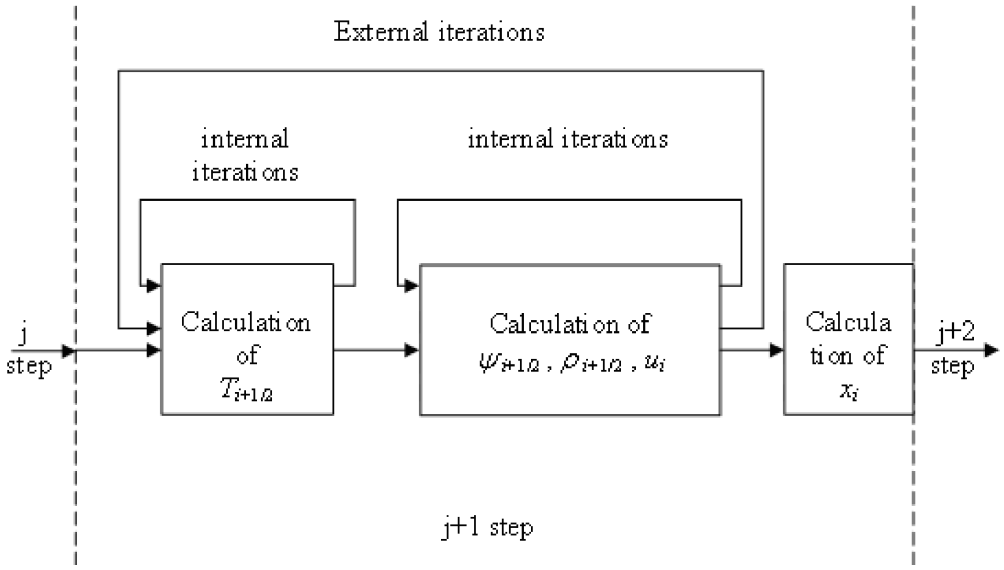

Fig. 6.1. Block-diagram of the iteration process on the time step

7. Results of the simulation

Figures 7.1 – 7.8 show the spatial velocity and density profiles for differential instants of time obtained from the solution of the Woodward — Colella method of dynamic adaptation with explicit separation of boundaries. All the figures show the solution obtained on a calculation grid with a total number of nodes $N = 420$ containing 80 cells in each internal region and 50

cells in each region adjoining the outer boundaries. By virtue of the given initial conditions (1.2), the evolution of each discontinuity will have its own singularities. In particular, the determining effect on the process as a whole is produced by the interaction of shock waves having different intensities. Figures 7.1 and 7.2 correspond to the instant of time when the left rarefaction wave has reflected from the outer boundary and approached the left shock wave, while the right rarefaction wave has only approached the opposite outer boundary. Further propagation of the shock waves towards each other leads to an even higher rarefaction in the regions between the shock waves and the outer boundaries. The density and velocity profiles are shown in Figs 7.3 and 7.4, and in Figs. 7.5 and 7.6 — the moment they collided. To the end of the calculation there corresponded the instant of time at which right shock wave has passed through the right contact boundary (Figs. 7.7 and 7.8), when all discontinuities characteristic of this time are clearly seen: two shock waves and three contact boundaries. It should be noted that solutions obtained by different methods with a total number of nodes less than 500 present only the quantitative behavior of the gas-dynamic functions, allowing quantitative errors, e.g., for the density, of about 50%. Figure 7.9 compares the density profiles calculated by the dynamic adaptation method to those obtained by means of the modified WENO scheme [11]. It is seen that the dynamic adaptation method has made it possible to obtain a solution on 420 cells practically coinciding with the solution on 12800 cells of WENO5m.

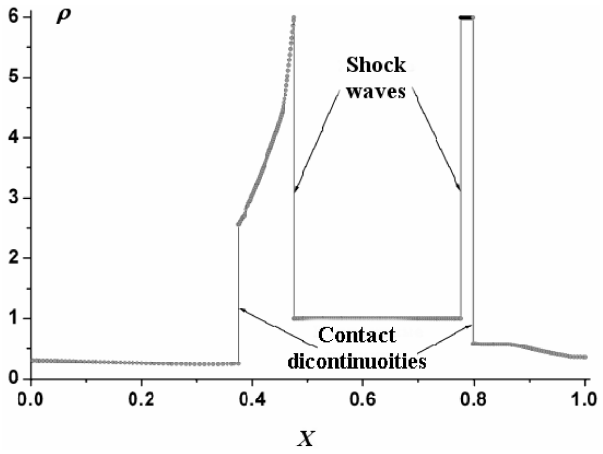

Fig. 7.1. Density profile at $t = 0.016$

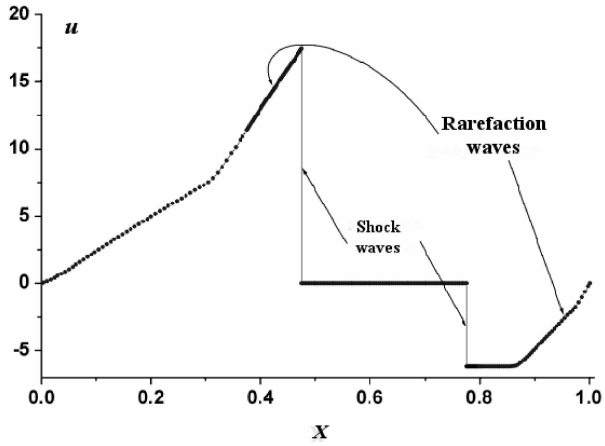

Fig. 7.2. Velocity profile at $t = 0.016$

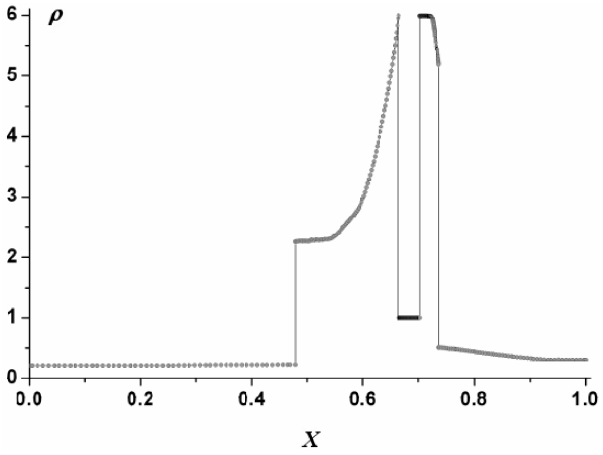

Fig. 7.3. Density profile at $t = 0.026$ before collision of the shock waves

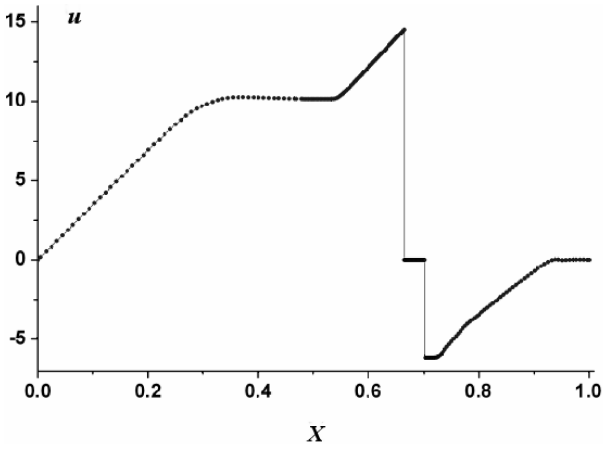

Fig. 7.4. Velocity profile at $t = 0.026$ before collision of the shock waves

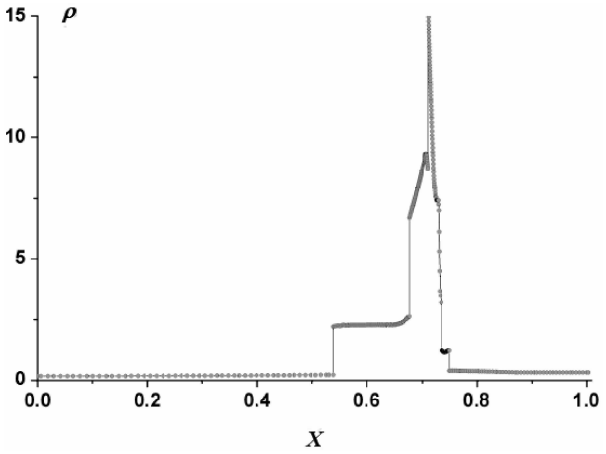

Fig. 7.5. Density profile at $t = 0.032$ upon collision of the shock waves

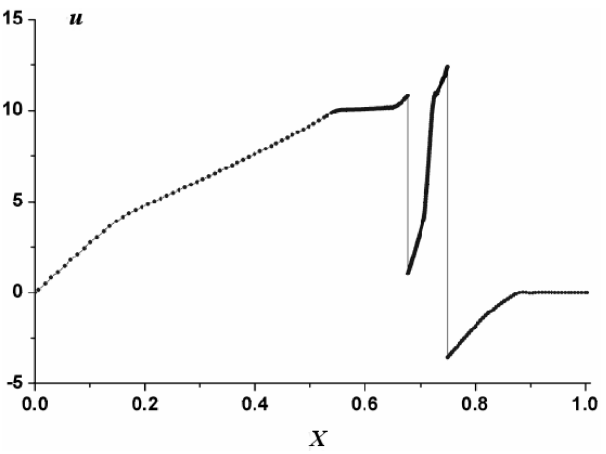

Fig. 7.6. Velocity profile at $t = 0.032$ upon collision of the shock waves

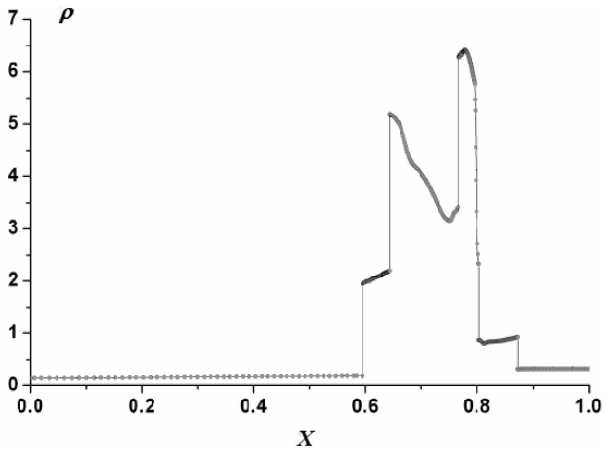

Fig. 7.7. Density profile at $t = 0.038$

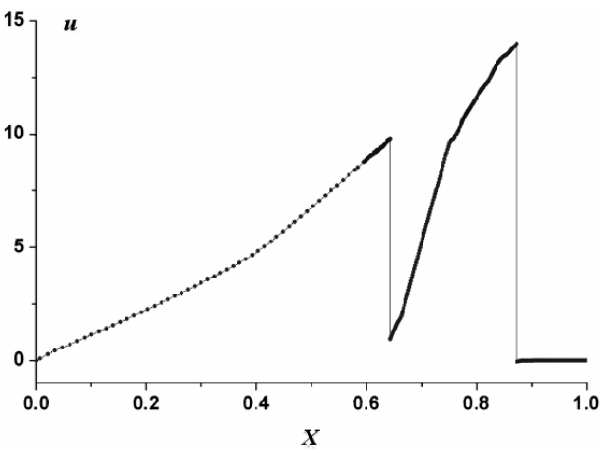

Fig. 7.8. Velocity profile at $t = 0.038$

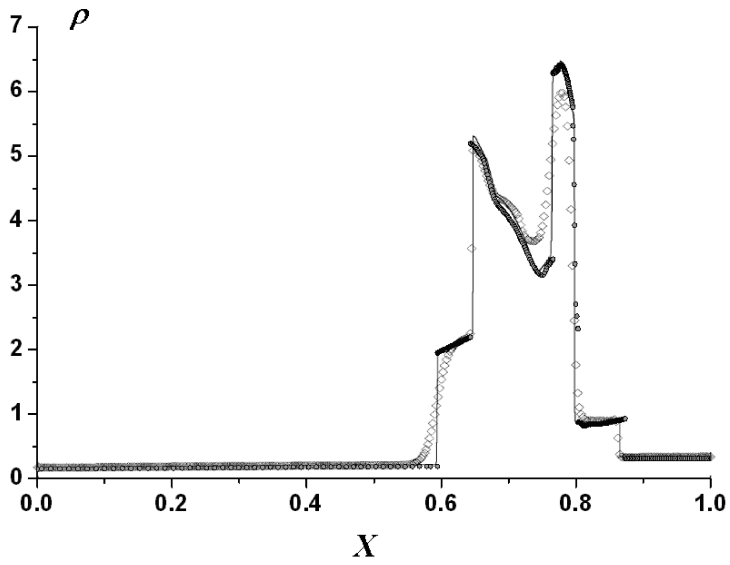

Fig. 7.9. Comparison between the solutions obtained by the dynamic adaptation method (• — 420 cells) and those obtained by WENO5m (◇ — 400 cells, solid line — 12800 cellss)

8. Conclusions

The dynamic adaptation method as applied to the problems of gas dynamics with multiple interactions of discontinuities that arise in the solution process has been considered. With the example of the test problem (Woodward — Colella problem) the efficiency and applicability of the proposed approach has been shown. The possibility of using the dynamic adaptation method for problems with multiple interactions of discontinuities, where their separation is needed, has been shown. As a transform function, an elementary diffusion-type adaptation function was chosen. The diffusion approximation in Woodward — Colella-type problems, where there is no need for nodes to crowd together towards the solution singularities has made it possible to construct quasi-uniform grids in all subdomains of the solution by choosing an adequate diffusion coefficient. The use of the dynamic adaptation method has made it possible to solve the Woodward — Colella problem on a grid with a total number of nodes reduced by a factor of 30.

References

1. B. N. Azarenok, *On one scheme of calculation of detonation waves on moving*, J. Comput. Math. Math. Phys., **45** (2005), no. 12, pp. 2260–2282.

2. Y. Bondarenko, V. V. Bashurov, and Y. V. Yanilkin, *A mathematical model and numerical methods for solving nonmstationary gas dynamic problems. Survey of foreign publications*, Preprint. RFNC-VNIIEF. 88-2003.

3. J. P. Boris, D. L. Book, and K. Hain, *Flux-corrected transport: Generalization of the method*, Journal of Computational Physics, **18** (1975), pp. 248–283.

4. P. V. Breslavsky and V. I. Mazhukin, *Mathematical simulation of the processes of pulsed diffusion and evaporation of a metal with explicit separation of the phase boundaries*, Journal of Engineering Physics and Thermophysics, **57** (1989), no. 1, pp. 107–114.

5. P. V. Breslavsky and V. I. Mazhukin, *The dynamic adaptation method in gas dynamic problems*, Matem. Modelirovanie, **7** (1995), no. 12, pp. 48–78.

6. P. Colella and P. R. Woodward, *The piecewise parabolic method (PPM) for gas-dynamical simulations*, Journal of Computational Physics, **54** (1984), no. 1, pp. 174–201.

7. N. A. Dar'in and V. I. Mazhukin, *On one approach to the construction of adaptive difference grids*, Doklady AN SSSR, **298** (1988), no. 1, pp. 64–68.

8. S. K. Godunov, *A difference method for numerical calculation of discontinuos solutions of hydrodynamic equations*, Mathematical book, **47** (1959), no. 3, pp. 271–306.

9. A. Harten, *High resolution schemes for hyperbolic conservation laws*, Journal of Computational Physics, **49** (1983), pp. 357–393.

10. A. Harten, *ENO schemes with subcell resolution*, Journal of Computational Physics, **83** (1989), pp. 148–184.

11. A. K. Henrick, T. D. Aslam, and J. M. Powers, *Mapped weighted essentially non-oscillatory schemes: Achieving optimal order near critical points*, Journal of Computational Physics, **207** (2005), pp. 542–567.

12. W. D. Henshaw, *A scheme for numerical solution of hyperbolic systems of conservation laws*, Journal of Computational Physics, **67** (1987), no. 1, pp. 25–47.

13. S. A. Ivananko and G. P. Prokopov, *Methods for construction of adaptive and harmonic grids*, J. Comput. Math. Math. Phys., **37** (1997), no. 6, pp. 643–662.

14. S. A. Ivanenko and A. A. Charakhchijan, *Curvelinear grids from convex quadrangles*, J. Comput. Math. Math. Phys., **28** (1988), no. 4, pp. 503–514.

15. O. N. Korolyova and V. I. Mazhukin, *Mathematical simulation of laser fusion and evaporation of multilayer materials*, J. Comput. Math. Math. Phys., **46** (2006), no. 5, pp. 910–924.

16. A. G. Kulikovskii, N. V. Pogorelov, and A. Y. Semenov, *Mathematical Problems of Numerical Solution of Hyperbolic Equations*, FIZMATLIT, Moscow, 2001.

17. R. J. LeVeque and K. M. Shyue, *One-dimensional front tracking based on high resolution wave propagation methods*, SISC, **16** (1995), no. 2, pp. 348–377.

18. V. D. Liseikin, *On some interpretaitions of a smoothness functional used in constructing regular and adaptive grids*, Russ. J. Numer. Anal. Modelling, **8** (1993), no. 6, pp. 507–518.

19. V. D. Liseikin, *Survey of the methods for constructing structural adaptive grids*, J. Comput. Math. Math. Phys., **36** (1996), no. 1, pp. 3–41.

20. X.-D. Liu, S. Osher, and T. Chan, *Weighted essentially non-oscillatory schemes*, Journal of Computational Physics, **115** (1994), pp. 200–212.

21. V. Mazhukin, A. A. Samarskii, and M. M. Chuiko, *The dynamic adaptation method for numerical solution of Stefan nonstationary multidimensional*, Doklady RAN, **368** (1999), no. 3, pp. 307–310.

22. V. I. Mazhukin, A. A. Samarskii, O. Kastelianos, and A. V. Shapranov, *The dynamic adaptation method for nonstationary problems with large gradients*, Matem. Modelirovanie, **5** (1993), no. 4, pp. 32–56.

23. V. I. Mazhukin, A. A. Samarskii, and A. V. Shapranov, *The dynamic adaptation method in the Burgers problem*, Doklady RAN, **333** (1993), no. 2, pp. 165–169.

24. E. Oran and J. Boris, *Numerical Simulation of Reacting Fluxes*, Mir, Moscow, 1990.

25. S. Osher, *Riemann solvers, the entropy condition, and difference approximation*, SIAM J. Numer. Anal., **21** (1984), no. 2, pp. 217–235.

26. L. V. Ovsyannikov, *Lectures on Fundamentals of the Gas Dynamics*, Computer Research Institute, Moscow, 2003.

27. D. V. Rudenko and S. V. Utjuzhnikov, *Application of grids dynamically adaptive to the solution for simulating spatial nonstationary gas flows with large gradients*, J. Comput. Math. Math. Phys., **42** (2002), no. 3, pp. 395–409.

28. A. A. Samarskii and Y. N. Popov, *Difference Methods for Solving Gas-Dynamic Problems*, Nauka, Moscow, 1992.

29. K. M. Shyue, *An efficient shock-capturing algorithm for compressible multicomponent problems*, Journal of Computational Physics, **142** (1998), pp. 208–242.

30. B. Van Leer, *Towards the ultimate conservative finite difference scheme. II. Monotonicity and conservation combined in a second order scheme*, Journal of Computational Physics, **14** (1974), pp. 361–376.

31. B. Van Leer, *Towards the ultimate conservative difference scheme. V. A second order sequel to godunov's method*, Journal of Computational Physics, **32** (1979), pp. 101–136.